

3.2 SUPERCONDUCTING COIL, REFRIGERATION SYSTEM, POWER SUPPLY AND CRYOSTAT

Introduction

To provide the desired momentum resolution the magnetic field inside the CDF tracking volume should be 1.5 T. This field can be produced by a cylindrical current sheet solenoid with a uniform current density of 1.2×10^6 A/M (1200 A/mm) surrounded by an iron return yoke. The CDF central electromagnetic calorimetry is located outside the coil of the magnet. This geometry requires that the coil be "thin" both in physical thickness and in radiation and absorption lengths.

Also, the solenoid and return yoke must be capable of being moved to and from the collision site and a nearby assembly hall where maintenance can be performed. An indirectly cooled superconducting solenoid with an external support cylinder has been designed¹ and built to meet these requirements. The solenoid and cryostat is about 3 meters in diameter, 5 meters long, 24 cm thick, with a total radiation length of .861, and a total absorption length of .194. The coil was designed by physicists and engineers from Fermilab, Tsukuba University and their vendor, Hitachi LTD, Japan. The coil was fabricated at Hitachi. The refrigeration system is a 600 W "stand-alone" version of the Fermilab ED/S satellite refrigerator and was built at Fermilab. The coil's power supply and controls system were also designed and built by Fermilab. For details beyond those contained in this description the reader is referred to the publications referenced at the end of this section.

Superconducting Coil and Cryostat

The coil for the CDF solenoid consists of a single layer helix winding of aluminum stabilized superconductor located inside a support cylinder and surrounded by radiation shields, superinsulation and vacuum shell. With the exception of the support structure and the Cu/Nb-Ti superconductor all material in the coil is made of aluminum. Table 3.2.1 gives the coil dimensions and design parameters. Table 3.2.2 gives the contribution of various components to the overall coil radiation and absorption length.

The CDF superconducting solenoid is adiabatically stabilized. The coil relies upon the heat capacity and high thermal conductivity of a high purity aluminum stabilizer to absorb and dissipate transient heat pulses in the conductor so that the superconductor remains below its critical temperature. Such heat pulses can be generated by conductor motion, cracking epoxy or other similar releases of mechanical energy. If the total energy release is sufficiently large, the conductor will quench. The coil is protected against this eventuality by insuring that the "quench wave" velocity is sufficiently high that the energy deposited in the coil is widely

distributed and thus can be absorbed without damage to the coil. Examples of other large solenoids of this type include those for CELLO, TPC, and CLEO.

The behavior of the coil following a quench has been computer modeled including the "quench back" effect of the eddy current in the outer support cylinder and the effect of the insulating layer between the coil and the outer support cylinder. Quench back was shown to be very effective in protecting the coil since the entire coil was calculated to be normal several seconds after quench initiation. With a $74 \text{ m}\Omega$ dump resistor the maximum expected conductor temperature is less than 100 K (see Fig. 3.2.3). The coil has five voltage taps to help locate quench origins. Heaters are installed to permit experimental quench studies.

An 1m diameter test coil of this type was fabricated and tested at Hitachi Ltd., Japan. A description of this coil and test results are given in the reference. In addition to the intrinsic coil design, additional coil protection is provided by the coil's power supply control system. This system, described in a later section, contains circuitry design to detail the initiation of a quench and remove as much of the magnet's 30 MJ of stored energy as possible by discharging the coil rapidly into an external dump resistor.

The conductor for the CDF coil consists of a monolithic copper/Nb-Ti matrix surrounded by a high purity aluminum stabilizer.

The conductor was produced by Hitachi, LTD using the extrusion with front tension (EFT) method.

A cross section of the conductor is shown in Fig. 3.2.1, and conductor parameters are summarized in Table 3.2.3. Figure 3.2.2 shows the short sample data for this conductor, together with the load line for the solenoid in the yoke. The conductor current density, at the 5-kA operating current of 64.3 A/mm^2 , is 60% along the load line to 4.4K. The conductor height is determined primarily by the maximum voltage to ground and the maximum temperature rise during a quench. The CDF solenoid has 10 conductor joints. Two conductor joints made using a new welding technique were tested successfully in the R&D solenoid. These conductor joints used a full turn of double layers of the normal conductor and two welded sections of 40 cm each, giving a net resistance of about $7 \times 10^{-10} \Omega$ at 4.2 K.

The solenoid will be installed in an iron flux return yoke the basic geometry of which is two calorimeterized end walls and four flux return legs. Calorimeterized poles extend into the solenoid field volume. The pole and end wall geometry determines the axial electromagnetic force on the coil and the radial and axial decentering forces. The axial force is calculated to be $\sim 1 \text{ MN}$ (compressive) at 1.5 T. The radial and axial force constants are computed as approximately 12 MN/m and 18 MN/m, respectively. The outward radial

pressure on the coil (0.9 MPa at 1.5 T) is reacted as a hoop stress in an outer support cylinder.

The cold-to-warm support system consists of six axial members, all on one end, to provide axial stiffness and 12 tangential members on each end to carry the cold mass and provide radial stiffness. These members are thermally intercepted at 77 K and 4.4 K to reduce the heat flux to the outer support cylinder and avoid hot spots. Spherical bearings on both ends of each member eliminate bending stresses due to differential thermal contraction.

The coil is refrigerated by two-phase helium at ~ 4.4 K flowing from a 2000-L storage dewar through ~ 130 m of 20-mm ID aluminum tube welded to the outer support cylinder. After cooling the outer support cylinder, the flow is used to intercept all the support members. The storage dewar pressure, maintained by the refrigerator, provides the driving force for the helium, i.e., the system does not have a pump. A finite element thermal analysis performed on the outer support cylinder gave a maximum temperature of 5.3 K.

The coil and support cylinder are screened from 300 K radiation by inner and outer liquid nitrogen cooled shields. End shields screen the coil ends and intercept the supports.

The vacuum shells are designed in accordance with the ASME Pressure Vessel Code. The outer shell is 20-mm thick; the inner shell is 7 mm. Since the inner shell has a critical collapse pressure differential ~ 0.02 MPa, the vacuum space is relieved by a 200-mm ϕ gravity liftoff plate.

A control dewar, located just outside the magnet yoke, provides the interface to the magnet cryostat. It has bayonet couplings for the cryogenic lines and a 55-L LHe reservoir fed from the helium return line. The superconducting leads from the coil enter the helium vessel through insulating feed-throughs and connect with gas cooled current leads leading to 300 K. Relief valves, a vacuum pumpout, and instrumentation connectors exit the system through the control dewar. A 200-mm ϕ x 3.5-m chimney connects the control dewar to the magnet cryostat. The control dewar, chimney, and cryostat have common vacuum. A cross section of the control dewar is shown in Fig. 3.2.4.

Coil and Cryostat Fabrication

The coil was fabricated by wrapping the conductor with B-stage Kapton tape and winding it with a tension of 980 N on a removable mandrel. An axial pressure of 10 MPa was applied and the coil heated to 135°C to cure the tape. In order to provide a uniform cylindrical outer coil surface to mate with the support cylinder, a layer of fiber reinforced plastic (FRP) was wrapped over the conductor, cured, and machined. The average thickness of the machined FRP layer was ~ 2.5 mm. The diameter of the conductor/FRP assembly was machined to within 0.1 mm of the desired dimension.

Sheets of 5083 aluminum alloy were rolled and welded to form a 3-m ϕ cylinder with a wall thickness of 16 mm except for a 44-mm thick section at each end 410 mm long to provide stiffness for the support system. After the outside surface of the cylinder was machined, a supporting fixture was attached to provide mechanical rigidity. The inner surface of the cylinder was then machined to a diametral accuracy of 0.2 mm. The radial interference between the coil and outer support cylinder was 1.5 mm. The calculation of the interference, based on considerations of conductor stress, winding strain, and cooldown effects, is given in Ref. 5. The outer support cylinder was heated to 100°C and lowered over the coil. The winding mandrel was then removed, giving a final radial preload of 0.27 MPa. A final axial compressive preload of 7.6 ± 1.5 MPa was applied to the coil by means of bolts in the support cylinder.

The vacuum cylinders were also fabricated by rolling and welding 5083 aluminum plates. The two annular end flanges were machined from 5083 plate. The radiation shields, 2-mm aluminum plates with a cooling tube welded on, were supported from the vacuum vessel with preloaded stainless springs.

The axial and radial supports were fabricated of Inconel 718; the axial elements were tubes 26 mm OD x 20 mm ID, the radials were 15 mm rods. The dimensions were chosen to provide a safety factor of four on the low-temperature tensile yield stress for a worst-case magnetic unbalancing. This system is shown schematically in Fig. 3.2.5(a). Figure 3.2.6 shows an individual radial support. The 6 axial supports are located at the power chimney end of the coil, and are designed to work either in tension or compression. There are 12 radial supports at each end of the coil connected approximately tangentially between the coil package and the vacuum vessel and preloaded to be always in tension. The coil position with respect to the vacuum chamber is fixed by these supports but the entire package can be shimmed axially if necessary. Similarly the radial position of the coil in the cryostat is fixed.

Differential thermal contraction of the coil in the radial direction is taken care of by allowing rotation about spherical bearings on the end of each radial and axial support.

The preload on the radial supports will be adjusted while the magnet is cold. Conduction heat leaks through the supports were calculated to be 0.25 W for each axial support and 0.31 W for each radial support for a total heat leak of 9 W. A cross sectional view of the coil and cryostat assembly is shown in Fig. 3.2.7.

The chimney and control dewar were fabricated of 18-8 stainless steel (Type 304), with aluminum-to-stainless transition couplings used on the fluid lines and the chimney vacuum jacket.

The superconducting leads from the coil to the gas cooled leads were fabricated of two pieces of coil conductor welded together. The positive and negative leads were clamped, through electrical insulation, to opposite sides of the helium supply line, which was immobilized by clamping to the outer support cylinder and to thermal stand-offs in the chimney. The ceramic feed-throughs at the bottom of the control dewar helium vessel were surrounded by a secondary vacuum vessel to guard the main vacuum system against helium leaks in the feed-throughs.

Extensive instrumentation was provided to monitor coil and refrigerator system behavior. Carbon and platinum resistance sensors were used; 9 in fluid lines and 26 on the coil, shields, and supports. There were 12 voltage taps on the leads and coil. Each of the 24 radial supports had a strain-gauge type force transducer, while the force in the axial supports was determined from axial position sensors. Thermocouple and cold cathode ion gauges monitored the main and secondary vacuum systems.

The coil was installed into the vacuum vessel (with its attached shields) in a vertical orientation. The final assembly is essentially all welded; the only o-rings are on the vacuum liftoff plate and the radial supports, where two rings are used with a provision for pumping the annular space between rings.

Refrigeration Requirements

The helium temperature refrigeration requirement of the solenoid cryostat and control dewar was calculated and measured to be ~ 40 W plus 14 L/h for the gas cooled leads. When the magnet is being charged to the design field of 1.5 T in 10 min there is an additional eddy current heat load of ~ 100 W. The transfer line, bayonets, u-tubes, and storage dewar contribute another heat load of ~ 30 W. The maximum total expected helium temperature refrigeration and liquefaction requirement is therefore ~ 170 W + 14 L/h. The refrigeration system should be adequate to permit operation with an unexpectedly high heat leak, and to permit rapid cooldown of the magnet. The Collider will perform physics experiments continuously for a six-month period, after which the 2400-ton detector will be moved from the collision area to a large assembly hall approximately 30 m away. The cryosystem must allow detector operation in both of these positions. The solenoid is designed to quench safely; but the refrigeration system must be capable of withstanding the associated pressure rise and provide a rapid recovery to superconducting temperatures.

Refrigeration System

The Fermilab satellite refrigerator⁷ was chosen as the basic component of the refrigeration system. The refrigerator consists of a 400 hp Mycom two-stage screw compressor, a four stage counterflow heat exchanger with liquid nitrogen precooling, and two expansion engines.

The satellite refrigerator is capable of operating as a liquefier only, refrigerator only, or at any point in between. The refrigeration/liquefaction capacity is shown in Fig. 3.2.8, with the shaded area indicating where the solenoid is expected to operate. It is seen that the refrigerator has a capacity which is generous compared with the anticipated load. This refrigerator was chosen primarily because the Fermilab Tevatron project has created a large body of experience in the operation and maintenance of the satellite refrigerator system. Spare parts and technical support are readily available to minimize system downtime.

Figure 3.2.9 shown the flow diagram for this refrigerator. Helium gas leaves the compressor at an absolute pressure of about 2.2 MPa (315 psia) and 270 K. Heat exchange with the returning stream cools the high pressure gas through HTX III, at which time ~ 65% of the input stream is expanded in the gas expansion engine and returned to counterflow. The remaining high pressure stream exits the heat exchanger at about ~ 25 K, and is expanded in the liquid engine to produce liquid at 186 kPa(abs) (27 psia) and 4.4 K. A J-T valve is available to provide some refrigeration should the liquid expander become inoperative.

Magnet Cooling Circuit

The flow diagram of the magnet refrigeration circuit, shown in Fig. 3.2.10, illustrates how the satellite refrigerator is integrated into the solenoid system. Refrigerator output is into a 2000 L storage dewar to provide the reservoir from which the magnet flow originates. From the dewar, flow is through one of two transfer lines to either the assembly or collision areas. A typical cross section of the transfer line is shown in Fig. 3.2.11. The helium flows from the transfer line into the control dewar subcooler, where it is cooled by the magnet return flow. After leaving the subcooler, the helium is expanded through a J-T valve and flows into the solenoid cryostat.

The magnet is cooled by approximately 130 m of 20 mm ID aluminum tubing welded to the outer support cylinder of the solenoid. Most of this cooling path is axially serpentine, with helium intercepts at all support attachment locations. A circumferential loop at each end of the solenoid provides additional end cooling. Upon leaving the magnet, the helium returns through the subcooler in the control dewar, the return (shell) side of the heat exchanger and to compressor suction.

Liquid nitrogen is supplied by a 12,000 L storage dewar and is used in two independently controlled circuits to cool the magnet support rod intercepts and the radiation shield. Nitrogen return flow from the magnet is used to shield the transfer lines and control dewar. Liquid nitrogen is also used for precooling in the refrigerator heat exchanger.

Refrigerator Control System

The control system is based on the Fermilab Tevatron system.⁸ A diagram of this system is shown in Fig. 3.2.10. The signals from pressure, temperature, engine speed, and other transducers are received by a Z-80 microprocessor in the multibus mainframe which performs the appropriate control functions. The multibus mainframe is linked through a CAMAC 080 module to the accelerator main control console from which the input and output variables, set points, and operating limits for valves and engine speeds can be easily changed.

The control loops associated with the solenoid refrigerator are identical with those in the Tevatron satellite installations. However, the loops controlling flow from the helium storage dewar to the magnet are unique.

The dewar liquid level is used to control both the liquid engine speed and the Joule-Thomson valve, EVJT, which in the absence of the liquid engine is capable of providing liquefaction, although with lower efficiency. The storage dewar pressure is used to regulate the amount of helium returned from the dewar by controlling valve EVBP. This pressure is also used to control EVBY, which acts as a relief valve.

The liquid helium flow to the magnet is regulated by controlling the subcooler pressure by means of EVHC on the helium return line in the transfer line. The setting of the J-T valve EVMC is done manually, and will be determined by monitoring magnet temperatures.

Power Supply and Power Supply Control System

The power components of the system consist of a 30 volt (limited to 20 volts), 5000 AMP Power Energy Industries power supply, an air-cooled free-wheeling diode, an LC power filter, a .004 Ω slow dump resistor, a slow dump switch, two fast dump switches, a .072 Ω fast dump resistor, and the 2.4 henry superconducting solenoid.

The P.E.I. power supply is the same as those in use in the FNAL experimental areas. It is a 12-phase type of SCR supply. A high precision transducer enables the control circuit to regulate the output current to within .05%.

The supply's internal free-wheeling diodes were replaced with an external air-cooled assembly. This allows for the free wheeling of magnet current during a power failure (i.e., no cooling water to the system).

To reduce the amount of noise going to the detector, an LC filter was specified. This filter is designed to reduce the voltage ripple from the power supply to about 500 mV peak-peak. Also included were common mode filter capacitors to reduce the ground referenced voltage ripple.

A slow dump resistor and switch is provided for non-critical system trips (i.e., any trip except quenches and high lead voltage). A slow dump trip will open the slow dump switch and turn off the power supply. This will force the current through the $.004 \Omega$ slow dump resistor and discharge the magnet with a time constant $T = 600$ seconds. This discharge time is sufficiently long that Eddy currents should not quench the coil under normal conditions.

Upon detection of a quench or high lead voltage, a fast dump trip is initiated by opening the fast dump switches. This forces the magnet current through the $.072 \Omega$ fast dump resistor. The fast discharge has an initial $T = 33$ sec. (The effective T will become shorter as the magnet coil quenches due to eddy current heating. The effective T at 5000 A should be 10-15 sec.)

A power supply Camac control crate is the heart of the system. It interfaces the power supply to the controller in the Tevatron Control Crate, allowing CDF local control, Tevatron control via the computer console, and manual control at the power supply. Also the interface allows the power supply to be interlocked by parameters critical to the safety of the system. Another interface controls the dump switches and examines the status and alarm switches in the system. A quench monitor compares symmetrical sections of the magnet in an analog voltage comparator circuit and will cause a fast dump trip if the voltages are not within 100 mV. Included in the power supply control crate is the interface for analog parameters which interlock and control the system. There are special analog to digital converter modules for logging purposes and a link controller to give this crate access to port B on the Tevatron control crate.

An IBM P.C. controls the power supply crate via an IBM/CAMAC crate controller. While the basic system control is hardwired, the IBM has responsibility for the logging process, networking thru port B (this allows the P.C. to log the He refrigerator parameters via Port B to the 080 module and to the M080 card in the multibus refrigerator control chassis), monitoring and displaying the performance of the system. The P.C. is an alternative to the Tevatron console for monitoring and control purposes.

Test of Refrigerator

The initial test of the refrigerator in March 1984 was to make liquid into the storage dewar. The refrigerator and dewar were cooled to liquid helium temperature in ~12 h. An electrical heater in the dewar was used to measure refrigeration and a superconducting-wire liquid level gauge was used to obtain liquefaction rates. The level probe, temperatures (VPT and carbon resistors), pressures, and expander speeds were monitored with the control system. Valves were operated, their positions monitored, and the various feedback loops stabilized through the control system.

The speeds of both gas and liquid expanders were adjusted for maximum refrigeration output at each heater power setting. The result of this test is given in Fig. 3.2.13. The capacity appeared to be somewhat in excess of the nominal value for the satellite refrigerator.

Initial Test of Solenoid

The first test of the solenoid was performed at the Hitachi Research Laboratory in the spring of 1984, with data recorded by representatives from the University of Tsukuba and Fermilab. Since this test was done without an iron flux return the current was limited to 2.8 kA. The coil was cooled down from room temperature to the LHe temperature in about 170 hrs. The resultant cooldown curve is given in Fig. 3.2.14. The resistance of the coil at ~10 K was measured to be 2 m Ω , which corresponds to an average RRR (residual resistivity ratio) = 1885. During the excitation tests the helium mass flow rate was 17 g/s, with a coil inlet temperature ~4.7 K and absolute pressure ~0.16 MPa.

A 100 m Ω dump resistor was used for the electrical tests. Temperature, current voltage, pressures were recorded by a data logger personal computer system and by several multichannel strip chart recorders. The excitation and dump schedule is given in Fig. 3.2.15. The maximum test current of 2.8 kA was chosen because at this current the axial magnetic force without iron is equal to the final compressive preload applied to the coil. The inductance without the yoke was measured during a charge as 1.92 H, so the stored energy at 2.8 kA was ~7.5 MJ. The coil reached the maximum test current at 100 A/min without a spontaneous quench.

The coil was ramped to 2 kA and back down at rates of 250, 333, and 400 A/min. Neither a quench nor a normal region was observed at these rates. The temperature increase of the outer support cylinder during the ramp was constant with time and is shown in Fig. 3.2.16. A series of induced quench tests using the heaters was attempted (Fig. 3.2.17). Adding ~10 kJ with three, 3.4-kJ pulses (340 W x 10 s) 14 s and 27 s apart did not cause an observable normal region at 2.8 kA. Further high power tests were not attempted because of the possibility of damaging the heaters and FRP insulation. Following the heater tests, the coil was operated at 2.8 kA for 10 h without incident. The stability of the coil was further demonstrated by stopping the helium flow with the coil at 10 A. After about 60 min the control dewar helium vessel boiled dry; about 10 min later the superconducting lead went normal. The entire coil went normal in about 10 min, an indication that there were no hot spots in the winding.

The obvious conclusion from the initial test is that at about 50% of the design field the coil is remarkably stable. Measurements indicate that charging the magnet to 1.5 T in 10 min is unlikely to

cause a quench with a helium flow rate of 17 g/s. The charging and quench behavior of the coil, with the complete iron circuit, to the guaranteed field of 1.35 T, and hopefully, to the design field of 1.5 T, as a function of helium flow rate, will be investigated in a comprehensive test program at Fermilab, beginning in Spring 1985.

Table 3.2.1

CDF Solenoid Parameters

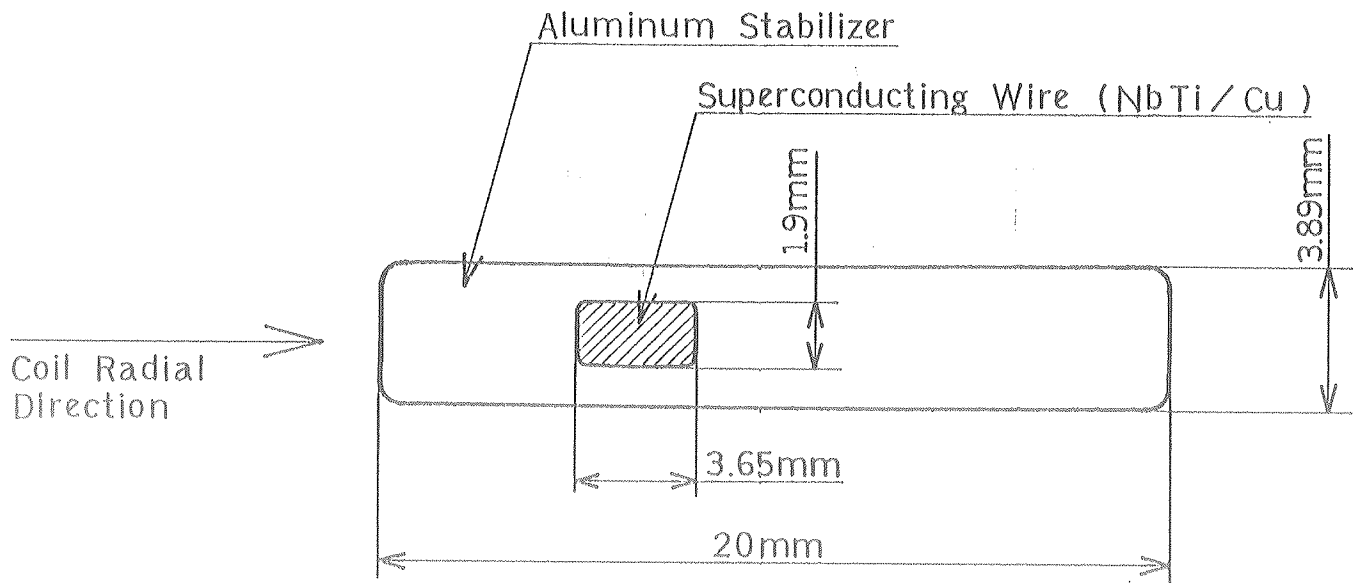
Outer Diameter	3351 mm
Inner Diameter	2857 mm
Overall Length	5067 mm
Coil Diameter	3014 mm
Winding Length	4792 mm
Axial Preload	7.6 \pm 1.5 MPa
Radial Preload	.35 \pm .07 MPa
Total Weight	13,000 Kg
Cold Mass	5,570 Kg
Central Field	1.5 T
Stored Energy	30 x 10 ⁶ J at 5000 A
Operating Current	5000 A
Inductance	2.4 H
Charge Time	20 minutes
Axial magnetic force on coil	~ 100 T
Axial magnetic decentering force	50 T/in
Radial magnetic decentering force	30 T/in
Steady state heat load (+ 100 W during 10 minute charge)	40 W + 14 l/hr

Table 3.2.3
Conductor Parameters

<u>Items</u>	<u>Value</u>
Filament Diameter	50 $\mu\text{m}\phi$
Number of Filaments	1700
SC Filament Area	3.34 mm^2
Cu/SC Ratio	1 : 1
Al/SC Ratio	21 : 1
Purity of Al matrix	99.99%
Measured RRR of Al	1885

References

1. R. Fast et al., "Design report for an indirectly cooled 3-m diameter superconducting solenoid for the Fermilab Collider Detector Facility, TM-1135", 1982, Fermi National Accelerator Laboratory, Batavia, Illinois.
2. T. Kishimoto, S. Mori and M. Noguchi, "Computer Simulations of Quench Properties of Thin, Large, Superconducting Solenoid Magnets", TSUKUBA-HEAP-5, May, 1982.
3. R. Wands et al., IEEE Trans in Magnetics, 1983, MAG-19, 1368-1371.
4. R. Fast, et al., "Refrigeration tests of the cryogenic system and solenoid for the Fermilab Collider Detector", Proc. 10th Intl. Cryo. Engr. Conf., Butterworth, London.
5. H. Minemura, et al., Nucl. Instr Meth, 1984, 219, 472-478.
6. R. Wands, et al., "Design of an indirectly cooled 3-m diameter superconducting solenoid with external support cylinder for the Fermilab Collider Detector Facility," IEEE Trans. Magnetics, MAG 19, 1368 (1983).
7. C. Rode, P. Brindza, and D. Richied, Energy doubler satellite refrigerator magnet cooling system, in: "Advances in Cryogenic Engineering, Vol. 25," Plenum Press, New York (1980).
8. J. C. Gannon, "Computer Operated Control System for the Energy Saver Satellite Refrigerators", TM-1024, Fermilab, Batavia, IL (1981).
9. R. W. Fast, et al., "Fabrication and testing of a 3-m diameter superconducting solenoid for the Fermilab Collider Detector", Proc. 10th Intl Cryo. Engr. Conf., Butterworth, Guildford.
10. Operations and Safety Manuals for CDF Superconducting Coil. (Fermilab) unpublished.
11. CDF Engineering Design Notes (Fermilab) unpublished.



Superconducting Wire | $50\mu\text{m}\phi \times 1700$
 Material Ratio | NbTi : Cu : Al = 1 : 1 : 21
 Aluminum Purity | $\sim 99.999\%$

Fig. 3.2.1. Aluminum stabilized conductor for CDF solenoid

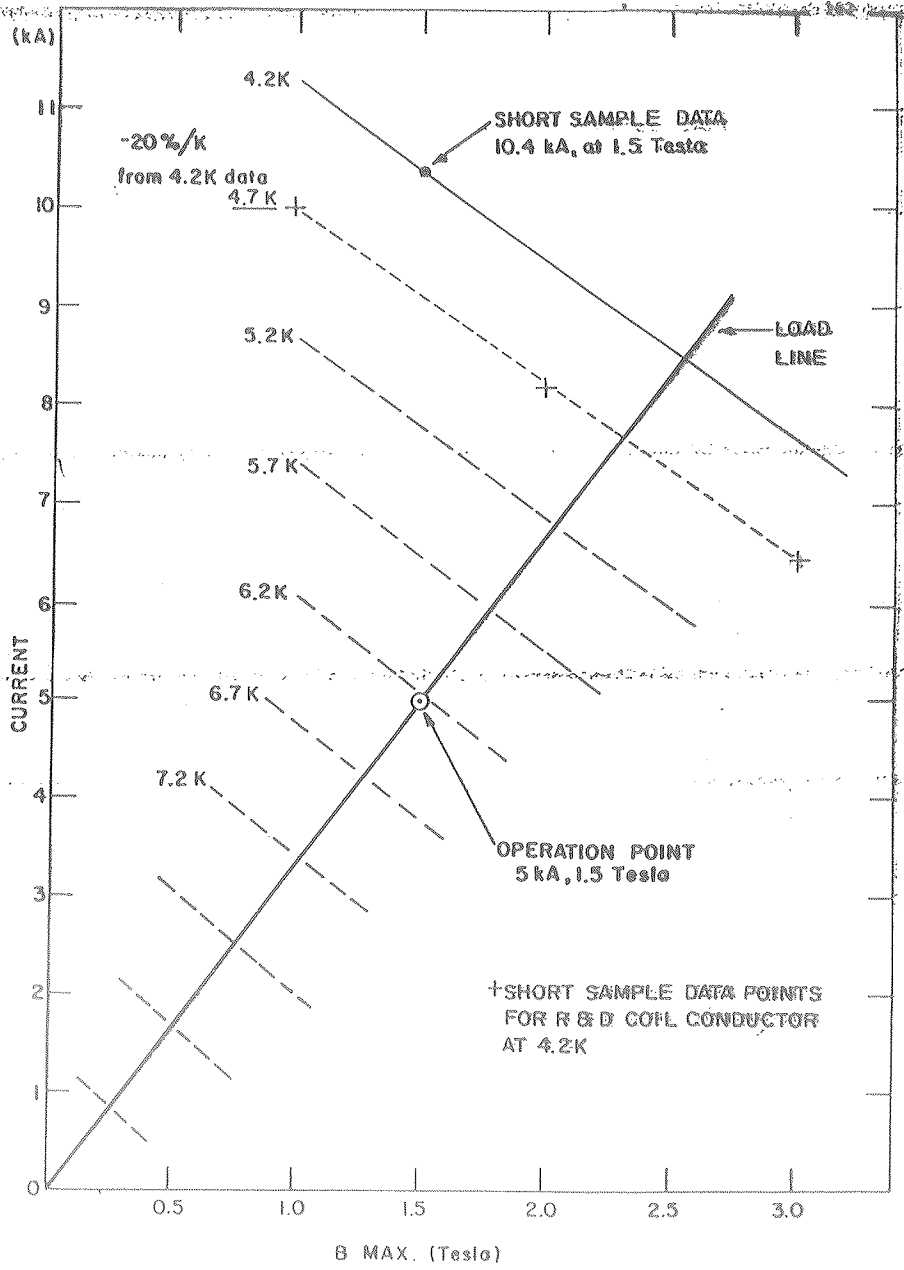
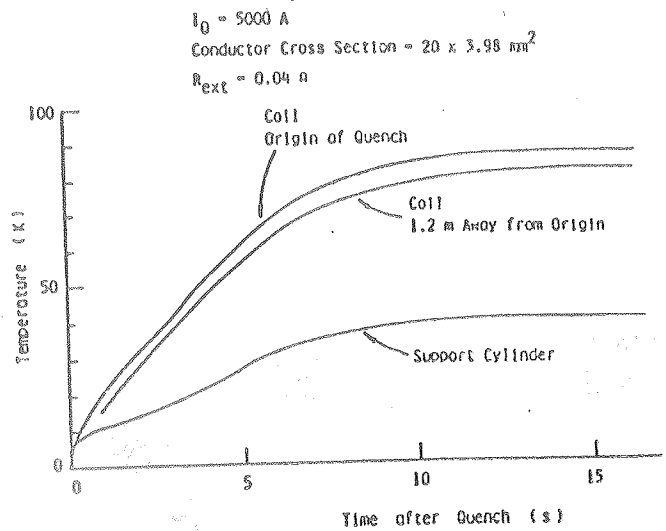
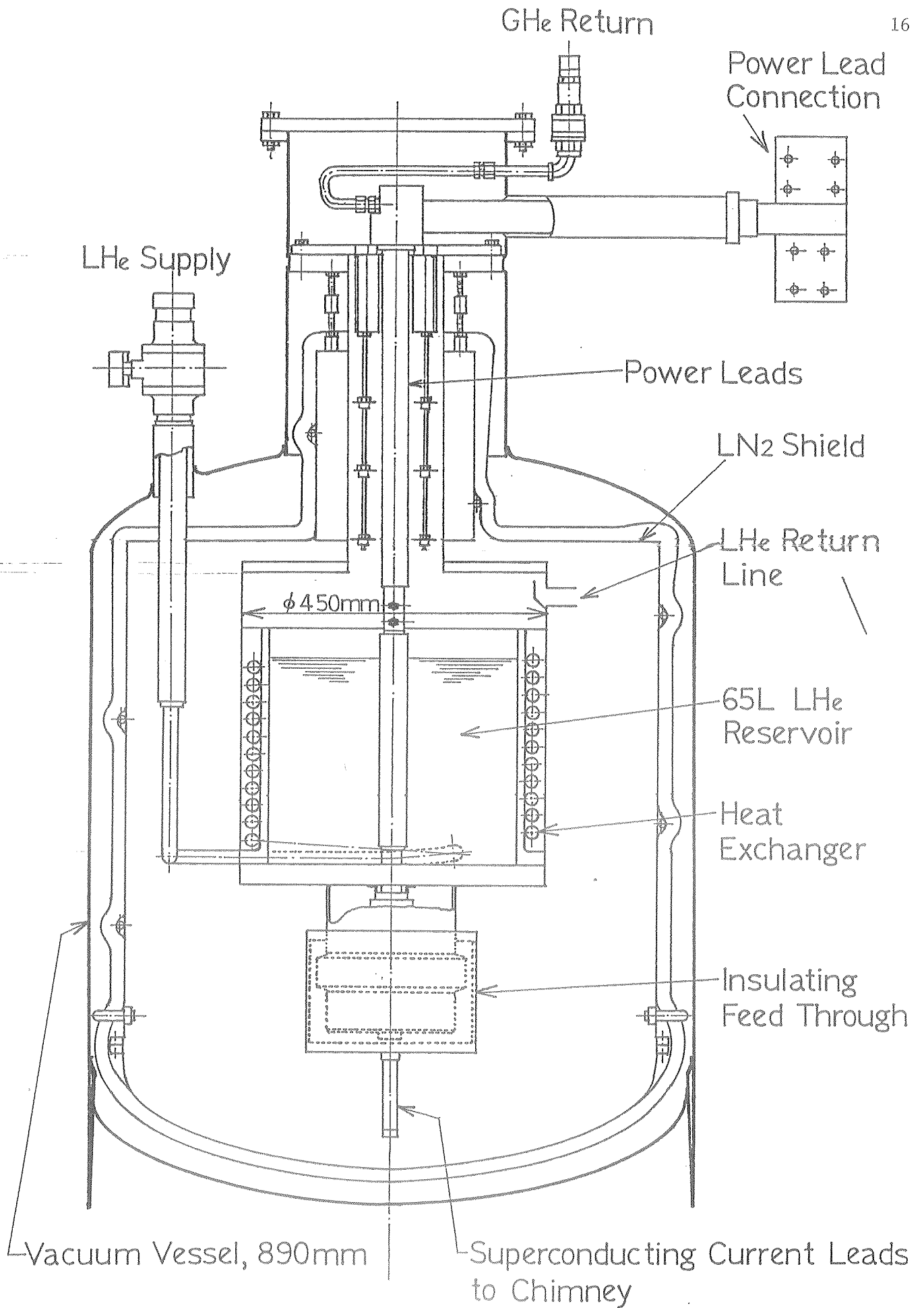


Fig. 3.2.2. Conductor performance as a function of temperature

Fig. 3.2.3. Temperature vs time following quench





- Fig. 3.2.4. Control dewar -

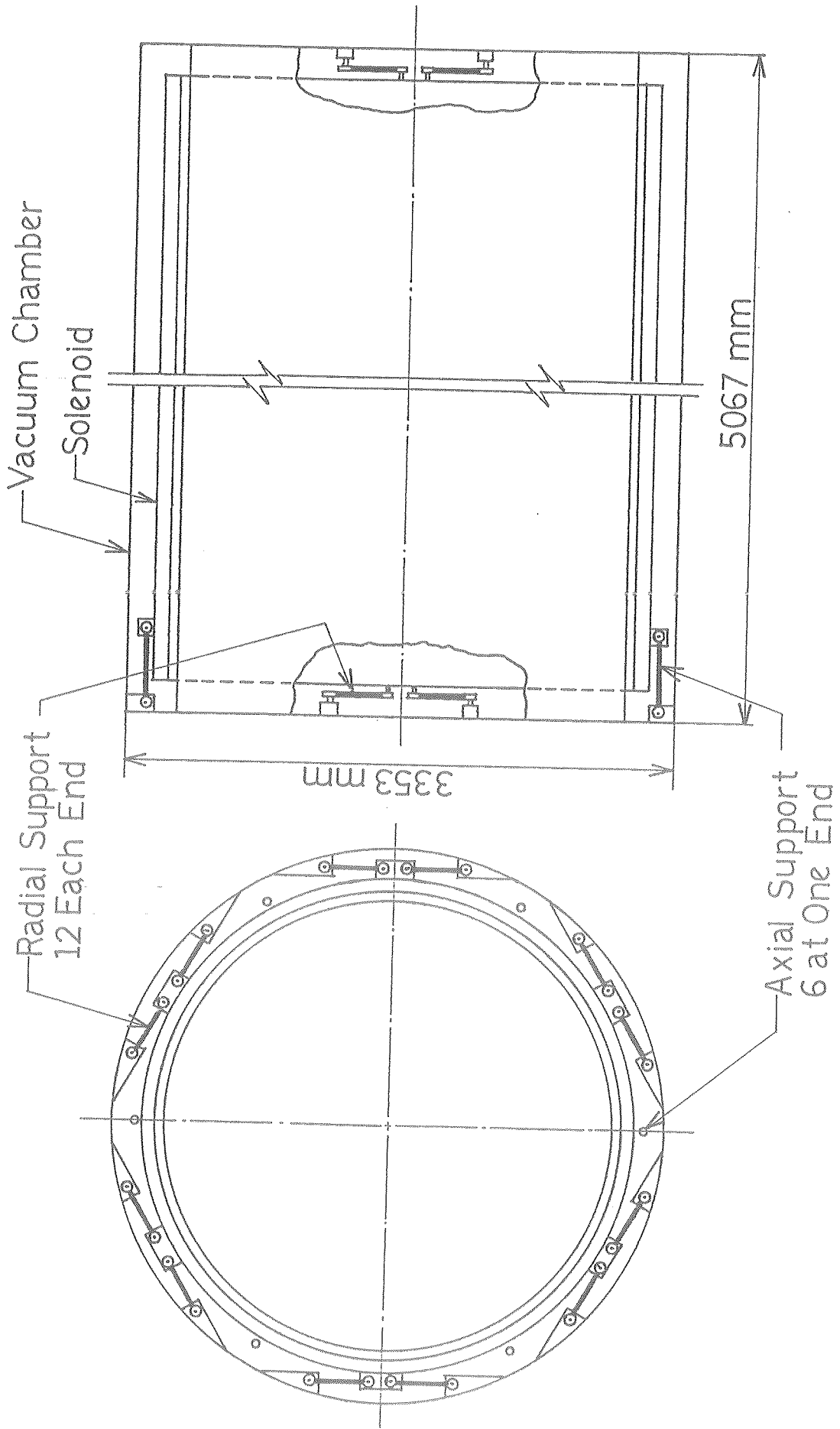


Fig. 3.2.5. Support system

All Dimensions in mm.

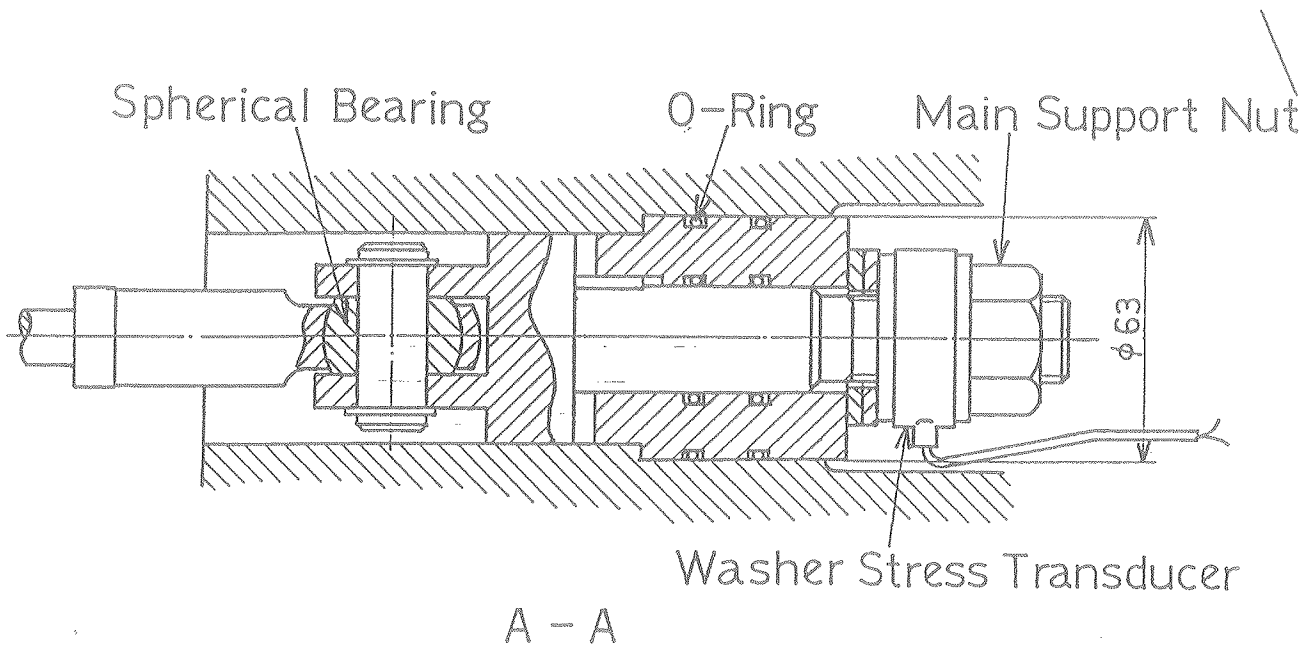
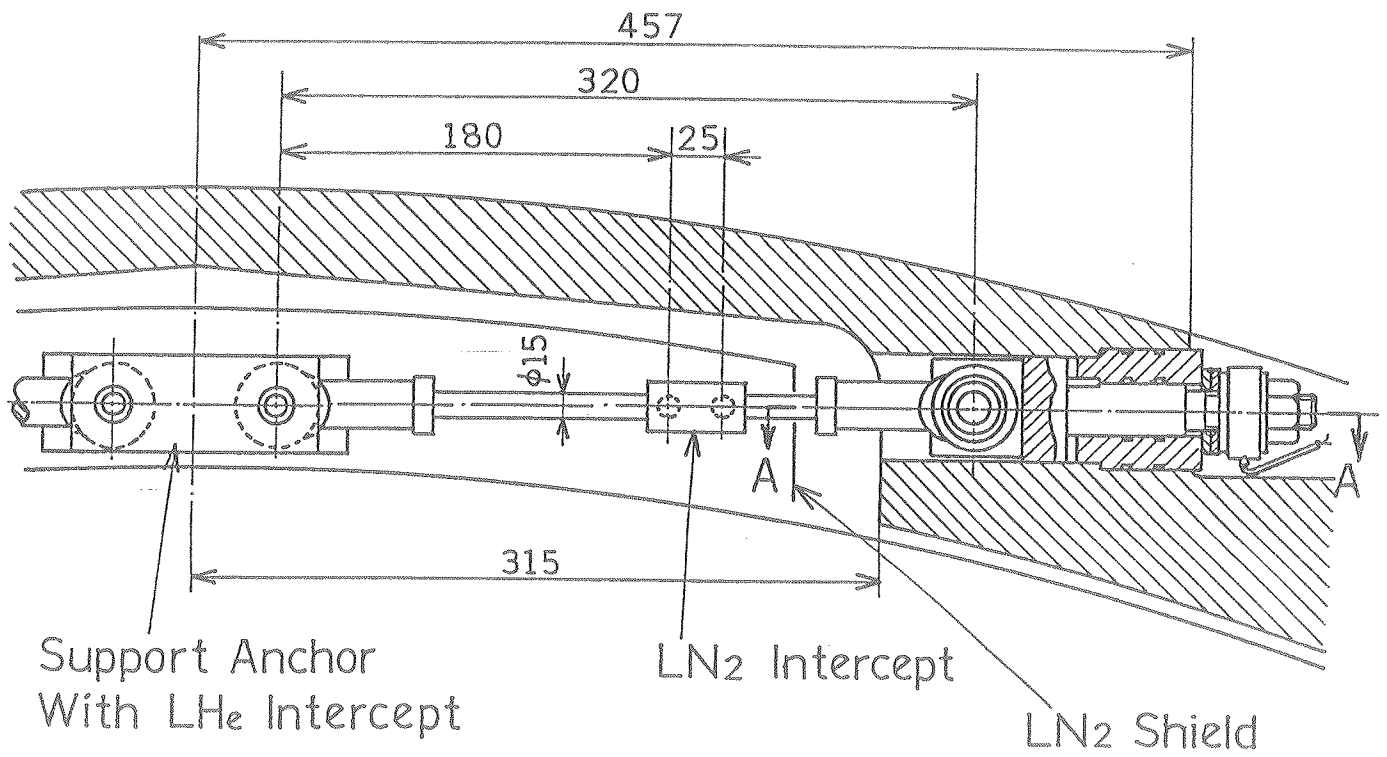
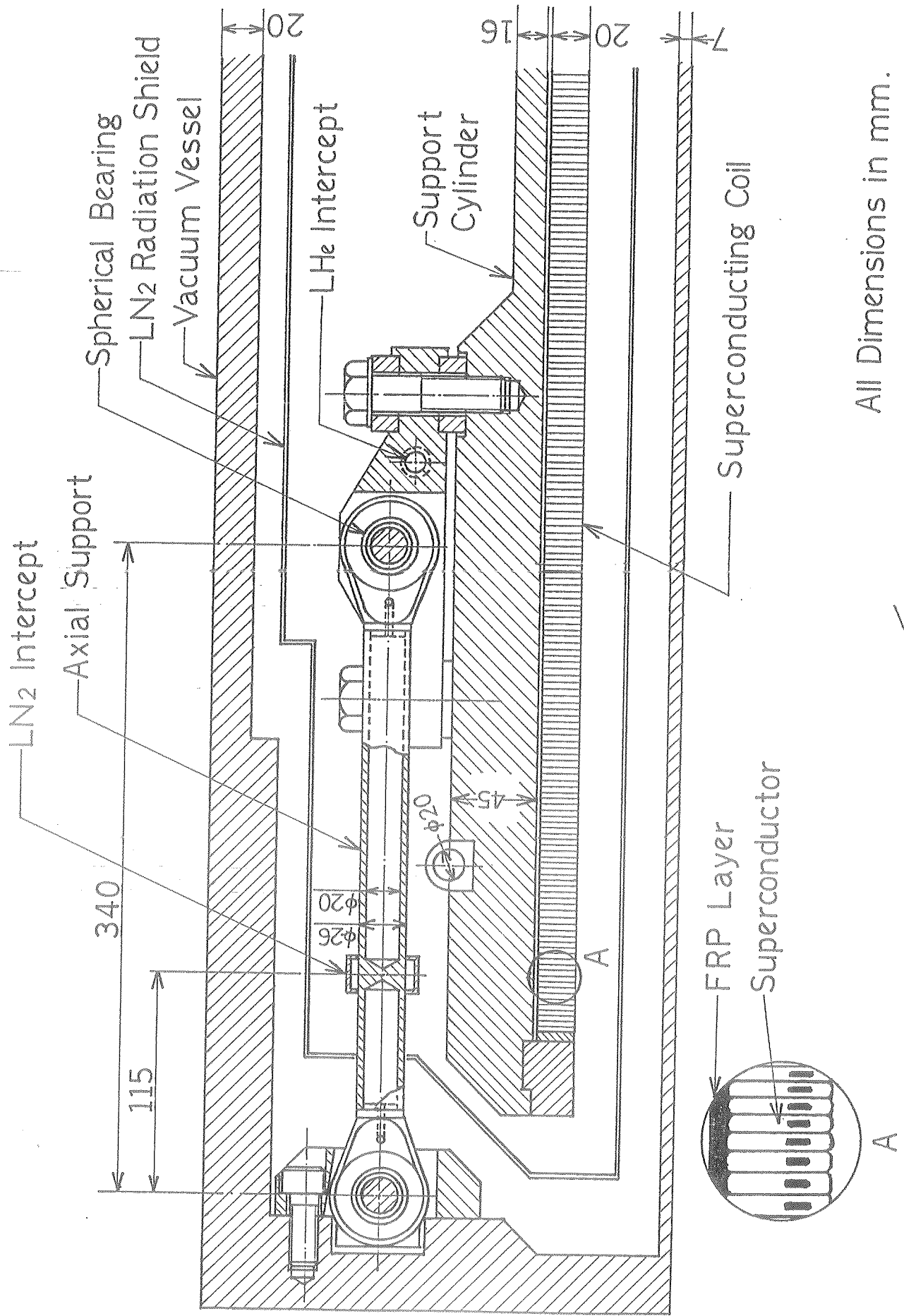


Fig. 3.2.6. Radial support rod



All Dimensions in mm.

Fig. 3.2.7. Axial support

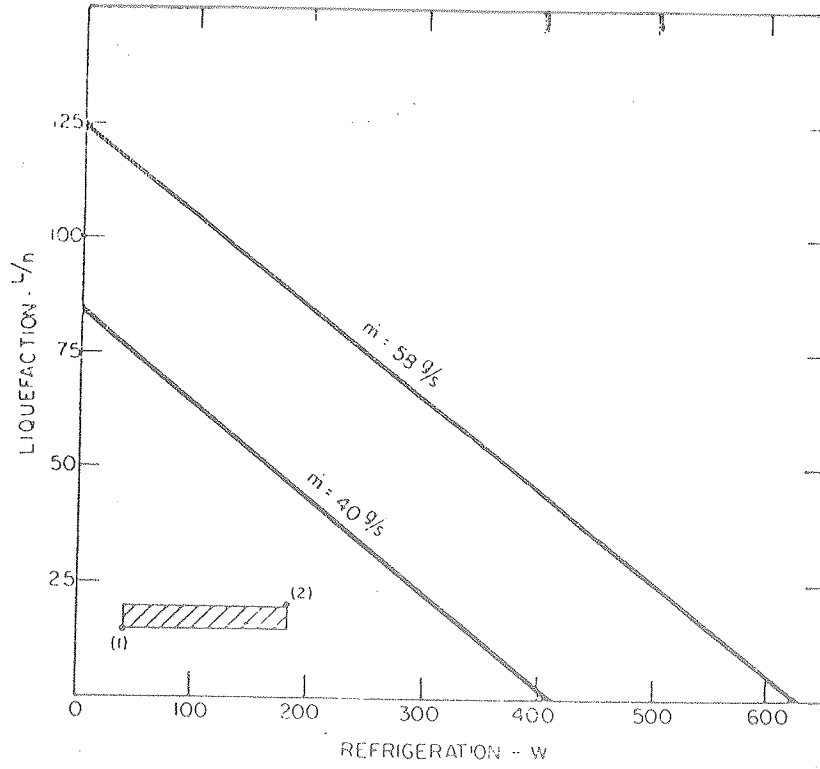


Fig. 3.2.8. Capacity of stand along refrigerator, identified steady state heat load (1), and maximum expected charging heat load (2).

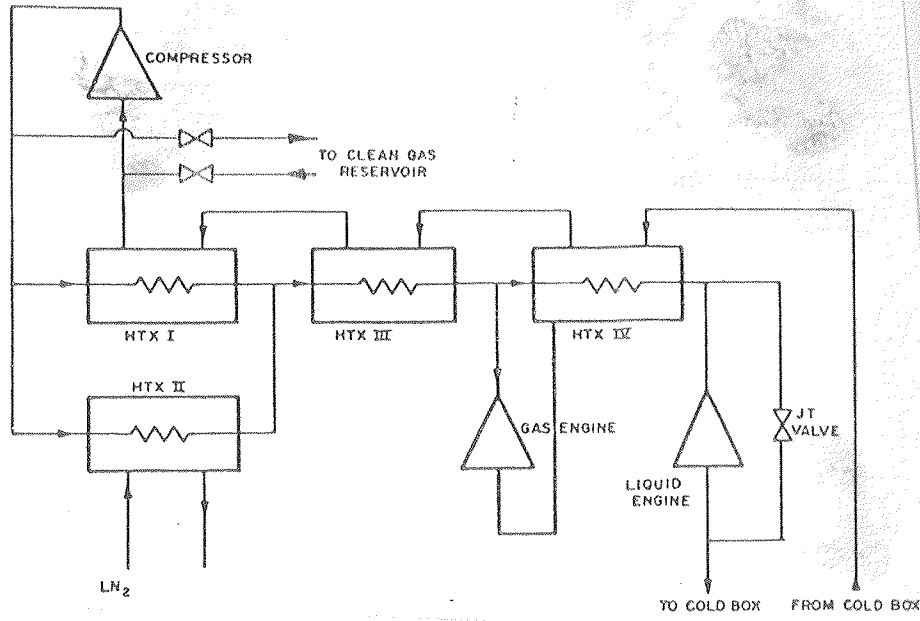


Fig. 3.2.9 Simplified Satellite Refrigerator Flow Diagram

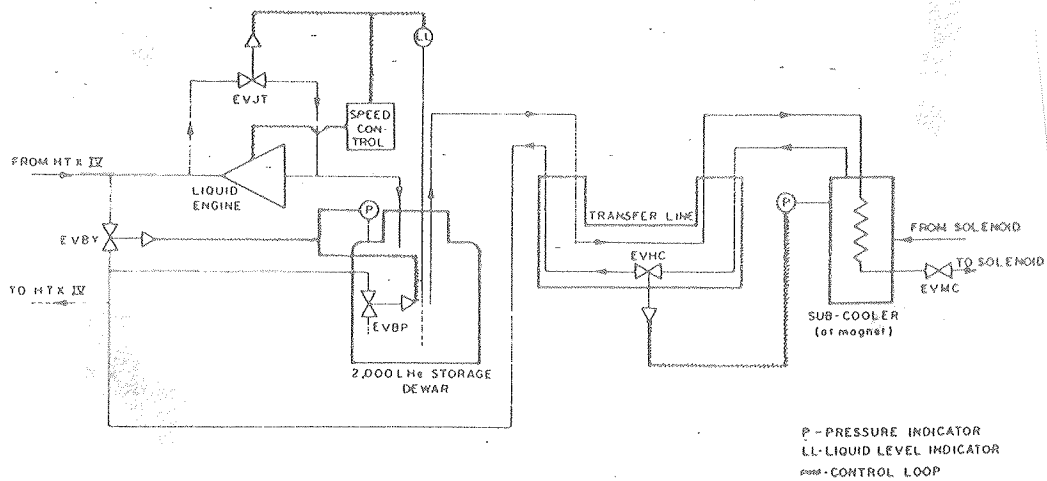


Fig. 3.2.10 Simplified Helium Flow Diagram

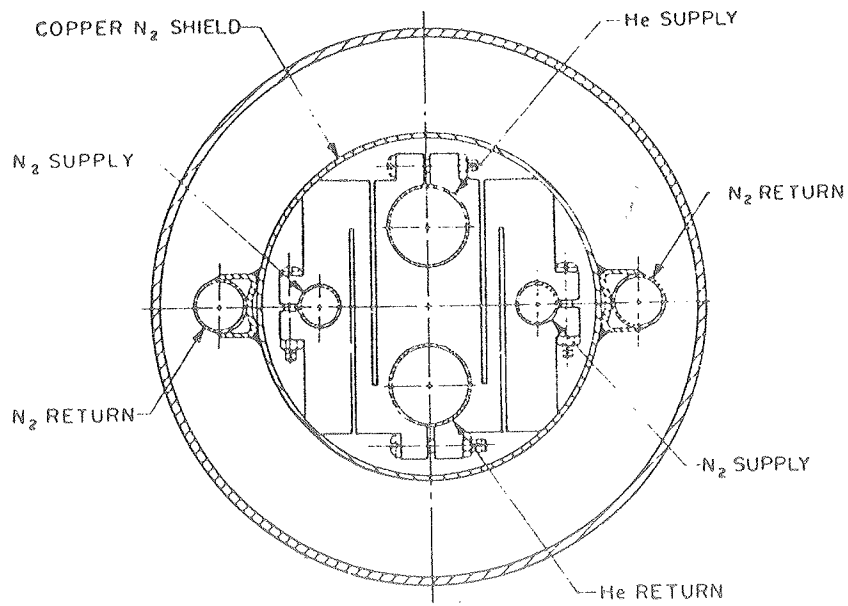


Fig. 3.2.11 Cross Section of Transfer Line

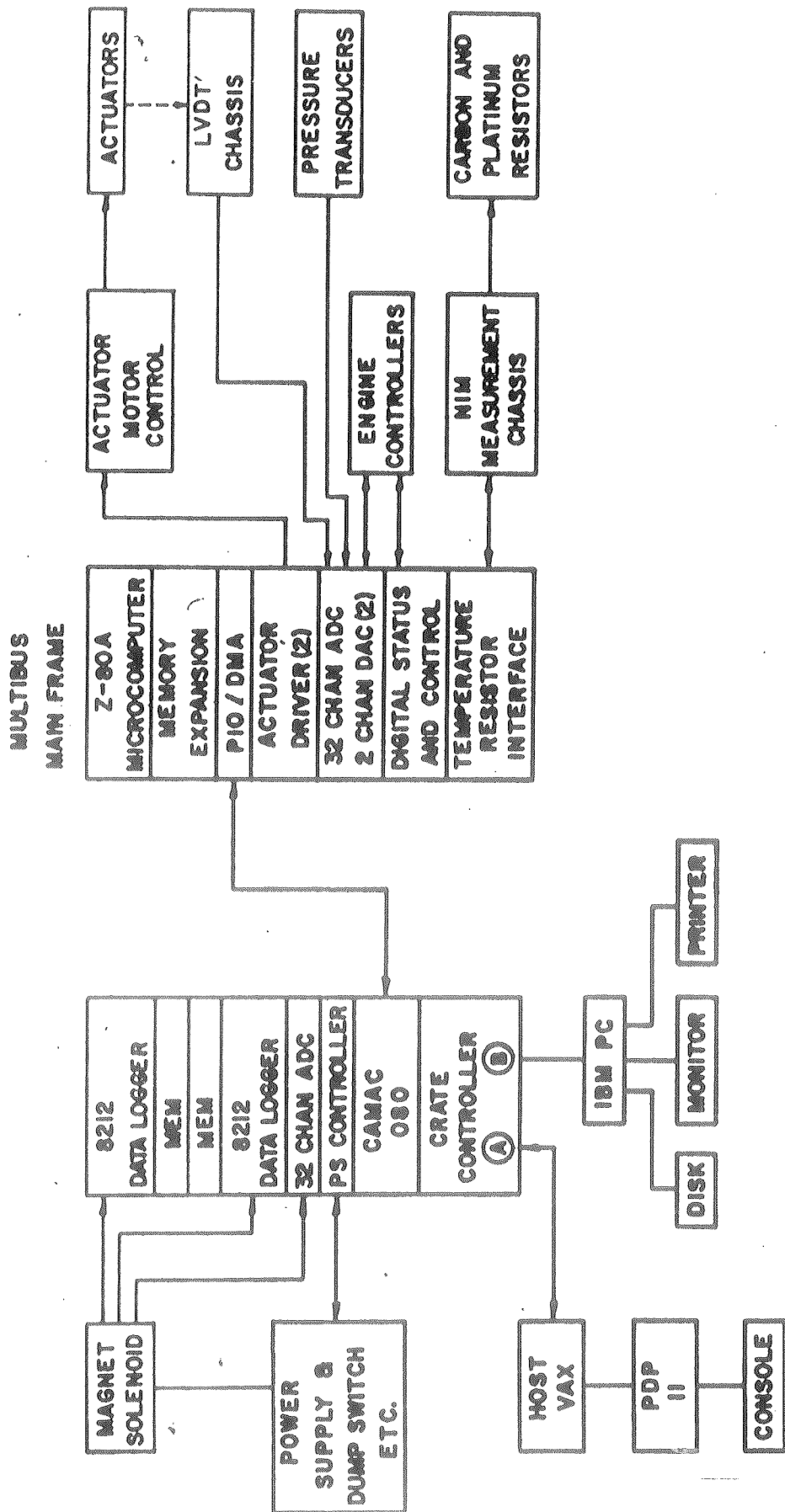


Fig. 3.2.12. CDF Satellite refrigerator controls block diagram

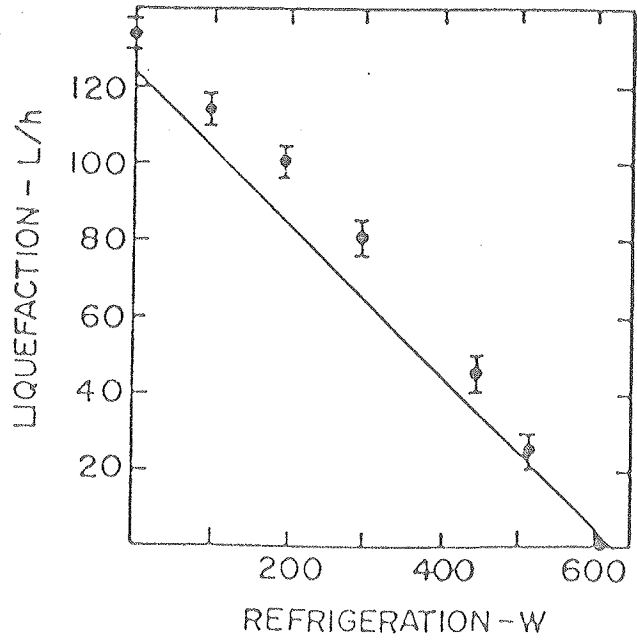


Fig. 3.2.13 Capacity of CDF Refrigerator

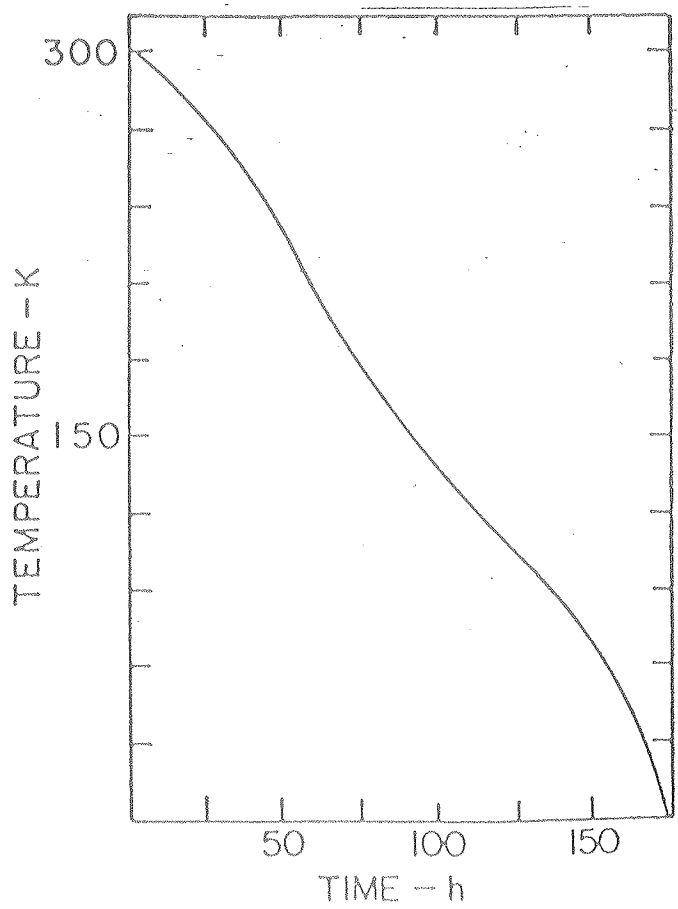


Fig. 3.2.14 Magnet cooldown - initial test at Hitachi

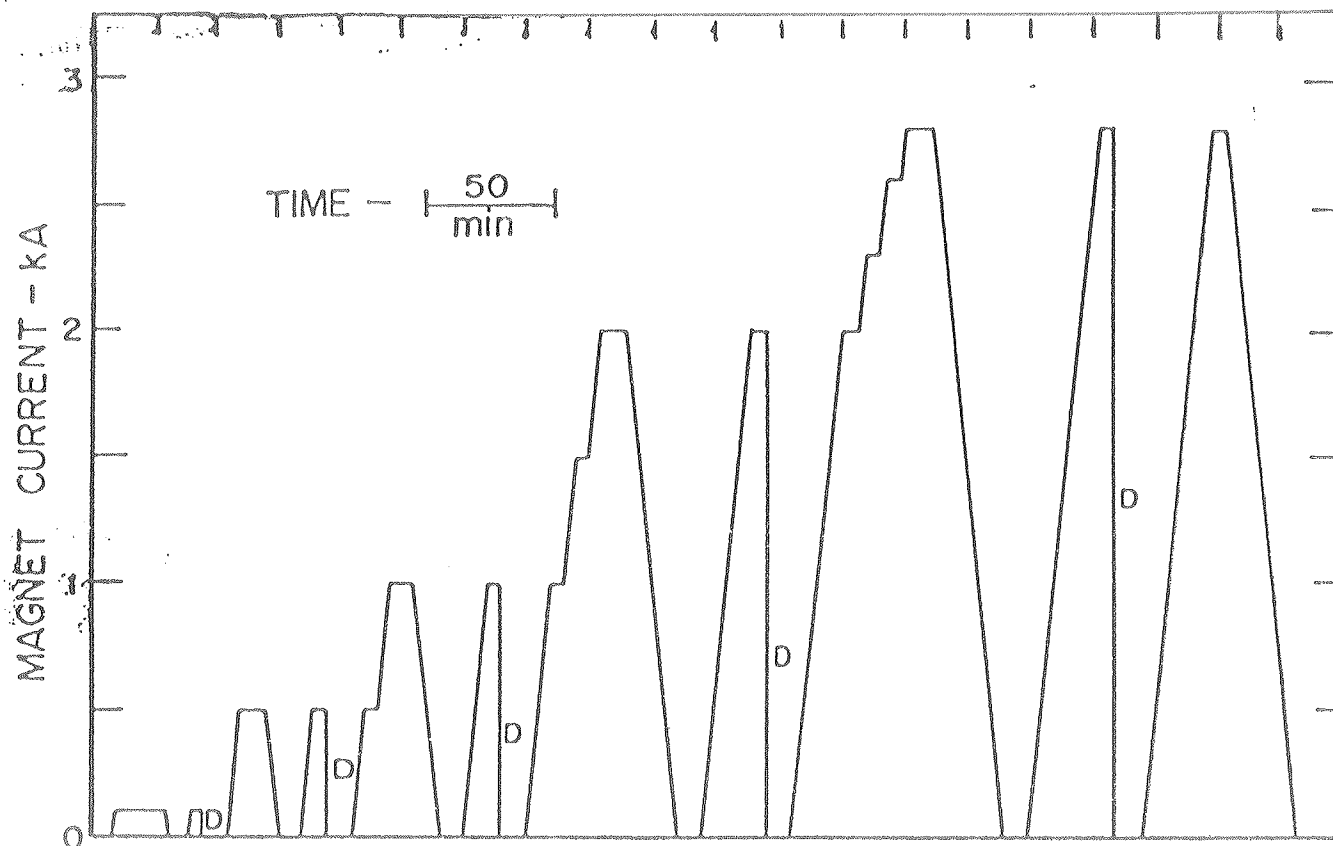


Fig. 3.2.15 Magnet excitation schedule. A dump discharge is indicated by D. Do not scale the time between successive charges.

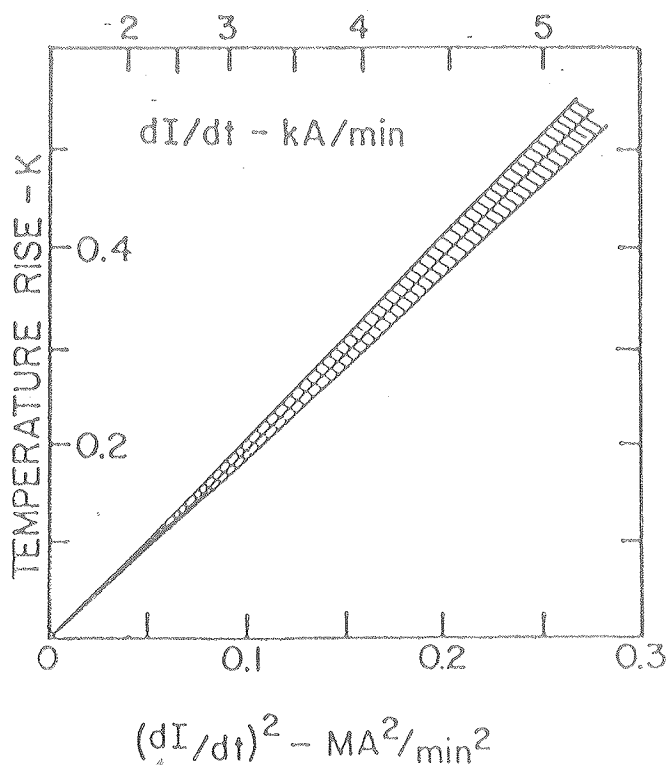


Fig. 3.2.16 The increase in the temperature of the outer support cylinder

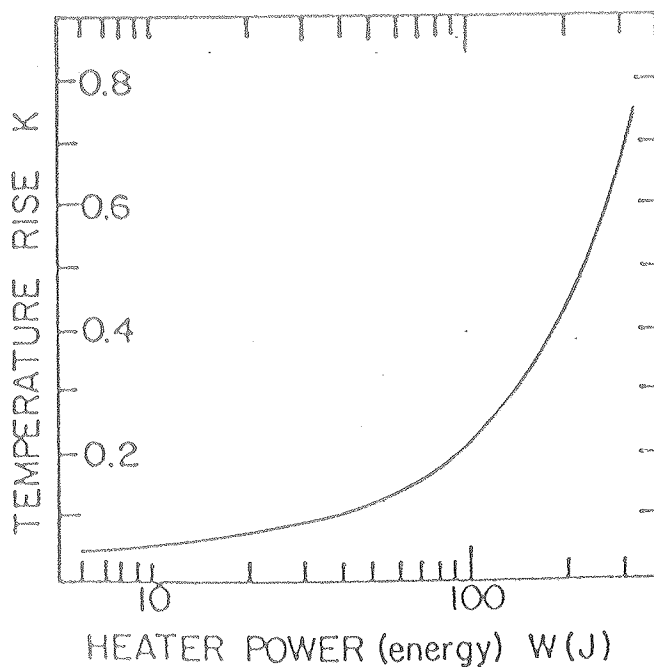


Fig. 3.2.17 The increase in the temperature of the outer support cylinder